

A topology preserving method for generating equilibrated polymer melts in computer simulations

Gopinath Subramanian^{a)}

Scientific Computation Research Center, Rensselaer Polytechnic Institute, Troy, New York 12180-3590, USA

(Received 22 June 2010; accepted 3 September 2010; published online 25 October 2010)

A new method for generating equilibrated configurations of polymer melts is presented. In this method, the molecular weight of an equilibrated melt of polymers is successively doubled by affinely scaling the simulation box and adding beads along the contour of the chains. At each stage of molecular weight doubling, compressive deformations are produced on all length scales, while the random walk nature of the polymers is preserved, thereby requiring relaxation times significantly smaller than the reptation time to fully equilibrate the melt. This method preserves the topological state of individual polymers in the melt and its effectiveness is demonstrated for linear polymers with molecular weight N up to 1024, and cyclic polymers with N up to 8192. For the range of N studied, the method requires simulation time that scales as N^2 and is thought to be applicable to a variety of polymer architectures. © 2010 American Institute of Physics.
[doi:10.1063/1.3493329]

I. INTRODUCTION

In polymer melts, the difficulty involved in directly observing entanglements, or directly measuring quantities such as the conformational free energy in an experiment makes computer simulations an indispensable tool. Coarse-grained molecular dynamics (CGMD) is an extensively used technique that can take advantage of parallel computing. Indeed, the Kremer–Grest bead-spring model¹ has been used to obtain the primitive path network,² calculate the tube potential,³ separate the roles of chain orientation and interchain entanglement in polymer glasses,⁴ study the development of entanglements in disentangled polymer melts,⁵ examine atomic stresses in polymer glasses,⁶ and investigate polymer crystallization.⁷ The starting point for most studies of polymer melts is a well-equilibrated system of entangled chains. A popular method of equilibration involves generating an initial configuration using a random walk or a self avoiding walk. This initial configuration is then allowed to evolve, as dictated by the Hamiltonian. The system is considered equilibrated after the polymer chains have diffused a distance comparable to their size. This brute-force method of equilibration is suitable only for relatively low molecular weights, as the longest relaxation time of an entangled polymer melt scales as the third (or higher) power of the molecular weight.

As a result, alternate techniques, such as Monte Carlo (MC) methods, are used to produce partially equilibrated configurations that are then fully equilibrated by CGMD. Examples of these MC methods include phantom chain growth by McKechnie *et al.*⁸ and geometric embedding by Müller *et al.*⁹ Other MC algorithms proposed by Vettorel *et al.*^{10,11} employ nonlocal moves such as kink translocation, whose validity has been questioned.¹² Some MC methods produce configurations with overlapping beads. The overlaps can be

removed using soft potentials, such as the modified Lennard-Jones⁸ or cosine potentials.¹³ Employing these soft potentials has been shown^{13,14} to deform longer chains, which relax only after they have diffused a distance comparable to their size.

The double-bridging algorithm proposed by Karayiannis *et al.*,¹⁵ and studied in detail by Auhl *et al.*,¹³ is a rapid equilibration method applicable to both lattice methods (such as the bond-fluctuation model),^{16,17} and CGMD methods (such as the bead-spring model). Double-bridging exchanges bonds between a pair of chains, thereby creating two new chains that can be substantially different from the original two. Intramolecular double-bridging is also possible, when bonds are exchanged between atoms belonging to the same chain. While double-bridging has been extended to H-shaped polymers,¹⁸ and three-arm stars,¹⁹ it is nevertheless difficult to extend double-bridging to polymers whose topological state must be preserved, such as cyclic polymers (CPs).

Other equilibration techniques, inspired by the dynamics of polymerization have been proposed.^{20,21} In these methods, the starting point is a dense melt of monomers, which are treated as radicals, and begin to capture other free monomers. Even with these methods, topology preservation is difficult.

In this study, a method for generating equilibrated configurations of polymer melts is presented. This successive molecular weight doubling (SMWD) method preserves the topological state of the individual polymers within the network. It was tested on both linear polymers (LPs) and CPs, but is general enough to be extended to polymers with other chain architectures, such as comb, H, pom-pom, and star. In the following sections, the model and procedures used for brute-force equilibration and SMWD are described. The structure of melts generated by both methods is characterized by measuring statistics of polymer dimensions, internal distance between beads, and the primitive path network. A re-

^{a)}Electronic mail: gsub@scorec.rpi.edu.

cently published scaling argument^{11,12} for the size of CPs in a melt is also confirmed: it is shown that the mean square radius of gyration of CPs in a melt varies as $R_g^2 \sim N^{2\nu}$, where as the molecular weight N increases, the exponent ν decreases from 0.4 and attains the limiting value of 1/3.

II. SIMULATION METHOD

A. Model

Polymers are represented using the coarse-grained bead-spring model¹ with beads of mass m . Excluded volume interactions are included through a Lennard-Jones potential given in Eq. (1).

$$U_{\text{LJ}}(r) = \begin{cases} 1 + 4\epsilon[(\sigma/r)^{12} - (\sigma/r)^6], & r \leq R_c \\ 0, & r > R_c. \end{cases} \quad (1)$$

The quantities σ and ϵ set the length and time scales of the simulations. The fundamental units of mass, length, time, and temperature are, respectively, m , σ , $\tau = \sigma(m/\epsilon)^{1/2}$, and $T = \epsilon/k_B$. The cutoff distance is chosen as $R_c = 2^{1/6}\sigma$, making the potential purely repulsive in nature. Consecutive beads on a polymer chain are connected by a finite extensible non-linear elastic (FENE) potential given in Eq. (2).

$$U_{\text{FENE}}(r) = \begin{cases} -0.5kR_o^2 \ln[1 - (r/R_o)^2], & r \leq R_o \\ \infty, & r > R_o. \end{cases} \quad (2)$$

The parameters were chosen to be $k = 30\epsilon/\sigma^2$ and $R_o = 1.5\sigma$. These parameters have been used in the past^{1,13} and ensure that the bonds between consecutive beads along a polymer are short enough, so that in conjunction with the strong repulsion between beads, chains are prevented from crossing each other.²² The equations of motion are integrated using a velocity Verlet algorithm with a timestep $\Delta t = 0.006\tau$. The temperature of the system is rescaled to unity every ten timesteps by rescaling the velocities of the beads in the system (drift of the simulation cell caused by this thermostat was on the order of $10^{-7}\sigma$, which shows that the so-called ‘‘flying ice’’ phenomenon does not develop in the time scales considered in this study). In subsequent sections, integration of the equations of motion along with the temperature rescaling is referred to as evolution. The number density of beads in the simulation box is $\rho = 0.85\sigma^{-3}$ throughout, except in the initialization stage for CPs, as described below.

B. Brute-force equilibration

A preliminary configuration for LPs was generated by growing them as random walks in a cubic simulation box with periodic boundary conditions. For CPs, the preliminary configuration was generated in a cubic simulation box large enough to accommodate all CPs without any overlaps between them. CPs were grown by placing beads along the circumference of a circle. The center of this circle was placed at a randomly chosen point in the simulation box and the plane of the circle was rotated to have a random orientation. CPs were placed in such a manner that the bounding cuboids of CPs did not overlap. Growing CPs as circles ensures that all CPs are the trivial knot, or unknot. Placing

them such that bounding cuboids do not overlap ensures that there are no catenated CPs. For CPs with $N = 1024$, the number density of the preliminary configuration was on the order of $10^{-3}\sigma^{-3}$.

The energy of the preliminary configuration for both LPs and CPs was minimized until the total energy of the simulation box dropped below $1 \times 10^{-30}\epsilon$. Following the energy minimization, the system was allowed to evolve for approximately 3×10^4 timesteps. In the case of CPs, the size of the simulation box was reduced during this run to attain a final length that yields a bead number density of $\rho = 0.85\sigma^{-3}$. The resulting system was taken to be the initial configuration. This initial configuration was allowed to evolve, and the autocorrelation of the end-to-end vector (for LPs), and the diametrical vector (for CPs) was monitored. These autocorrelation functions are defined in Eq. (3).

$$p_i(t) = \frac{\langle \mathbf{R}_{ee}(t) \cdot \mathbf{R}_{ee}(0) \rangle}{\langle R_{ee}^2(0) \rangle}. \quad (3)$$

For LPs ($i=L$), p_L is obtained by setting $\mathbf{R}_{ee}(t) = \mathbf{R}_N(t) - \mathbf{R}_1(t)$, the vector connecting the end beads of an LP. For CPs ($i=C$), p_C is obtained by setting $\mathbf{R}_{ee}(t) = \mathbf{R}_{N/2}(t) - \mathbf{R}_1(t)$, the diametrical vector of a CP. At any given time t , the diametrical vector of a CP was computed using the position vectors of the same two beads that were used to compute the diametrical vector at $t=0$. Systems were considered equilibrated when $p_i(t)$ had decayed past zero.

C. Successive molecular weight doubling

The SMWD method is a multistage process. A fully equilibrated system with molecular weight N_{old} is taken to be the initial configuration for each stage. Each stage consists of scaling and equilibration. The scaling is shown schematically in Fig. 1 for a single LP and a single CP. Here, the simulation box of the initial configuration, along with the polymers, is scaled affinely by a factor of $2^{1/3}$. This affine scaling yields the new coordinates (x', y', z') of an arbitrary point (x, y, z) according to $(x', y', z') = 2^{1/3}(x, y, z)$. This scaling ensures that the length of every arbitrary vector in the simulation box is multiplied by the scaling factor, and that the angle between every arbitrary pair of nonzero vectors remains unchanged. Thus, the affine scaling preserves the topology of the entanglement network.

In this scaled simulation box, every polymer is replaced by a new polymer of molecular weight $N_{\text{new}} = 2N_{\text{old}}$, by placing beads of the new polymer along the contour of the old polymer. The normalized coordinate along the contour of the scaled old polymer is denoted by s . For LPs, $s=0$ corresponds to one end bead, and $s=1$ corresponds to the other end bead. N_{new} equally spaced beads are then placed over $s \in [0, 1]$. For CPs, $s=0$ and $s=1$ both denote the bead that was designated as bead 1 in the simulations. $N_{\text{new}} + 1$ equally spaced beads are then placed over $s \in [0, 1]$. The bead corresponding to $s=1$ is removed, as it is identical to the bead with $s=0$. The bonds of the new polymers are then updated appropriately.

The affine scaling and adding beads is a synthetic construct that has been used, as far as the author is aware, for the

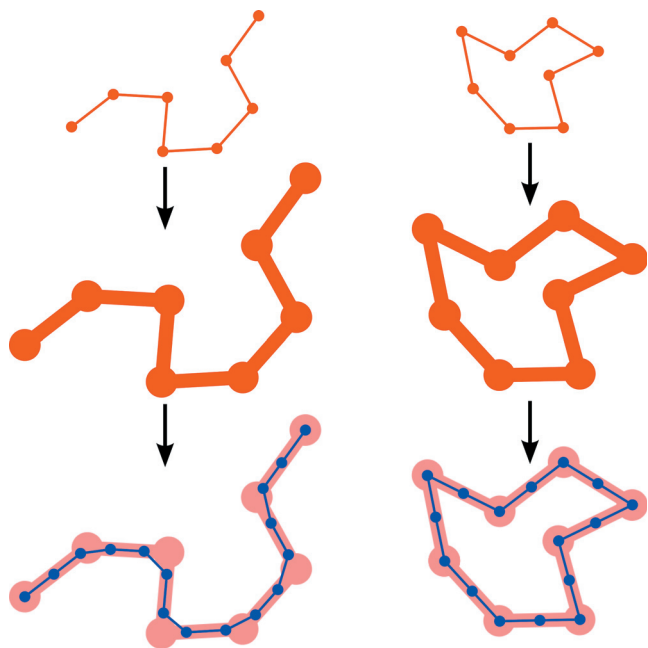


FIG. 1. Schematic of the SMWD method applied to LPs and CPs for $N_{\text{old}} = 8$. The original polymers at the top (red) are affinely scaled and replaced by new polymers (blue) with $N_{\text{new}} = 2N_{\text{old}}$. In CPs, since the number of bonds is equal to the number of beads, the contour of the new CP exactly follows the contour of the scaled old CP.

very first time, as a device for rapid equilibration. It is inspired by the chain explosion process described by deGennes,²³ where upon rapid melting, a crystalline polymer with a low entanglement density reaches equilibrium in a time that scales as $N^{1/2}$. Nevertheless, it must be mentioned that the effect of molecular weight on the chain explosion process is a subject of some debate. Experimental studies^{24–26} suggest that slow melting of a disentangled melt leads to formation of the “heterogeneous melt” state, which relaxes in a reptation time, while computational studies, using both the Bond fluctuation model,²⁷ and the Kremer–Grest bead-spring model⁵ have not been able to convincingly replicate this phenomenon. This might be in part because the heterogeneous melt state is observed for high molecular weight polymers, which are computationally expensive to model.

The construct used in the present study generates a new simulation box with the same density ($\rho = 0.85\sigma^{-3}$) as the old one, assured by the choice of scaling factor. The random walk nature of the polymers is preserved, albeit with a different step length. The entanglement density, on the other hand, is reduced by a factor of 2. The end-to-end vector of the new polymers is scaled by a factor of $2^{1/3}$, which results in compressed LPs, and compressed low molecular weight CPs. This synthetic construct does not correspond to any real phenomenon and is used to bypass the long relaxation times associated with polymer melts. For CPs, the scaling of polymer size produced by the affine scaling is consistent with the natural scaling of CP size^{11,12} for large molecular weights, and thus relaxations are required only on the smaller length scales. LPs, on the other hand, are deformed at all length scales, but the lowered entanglement density is expected to produce an acceleration in the equilibration time. However,

as was rightly pointed out by a reviewer, the time required to fully equilibrate a melt of affinely scaled LPs is somewhat uncertain. In this study, the period for which equilibration of the affinely scaled polymer melt is performed is referred to as the transition period. For CPs, which have faster dynamics,²⁸ the transition period was set to be $1.5\tau_R$. For LPs, the transition period was set to be $5\tau_R$. It will be shown that this duration of the transition period is sufficient for equilibrating the molecular weights considered in this study. The melt produced at the end of the transition period then serves as the initial configuration for the next stage of doubling. The procedure is repeated until the desired molecular weight is reached.

The Rouse time was computed as $\tau_R = \tau_e(N_{\text{new}}/N_e)^2$. Here, τ_e is the relaxation time of an entanglement segment and N_e is the number of beads between entanglements. These latter quantities were estimated from melts of LPs generated using the brute-force method. By assuming that the reptation time for LPs with molecular weight N is equal to the time taken for $p_L(t)$ to decay to zero, the relaxation time of an entanglement segment was estimated as $\tau_e \approx 10^4\tau$. From the primitive path analysis of equilibrated LPs, the number of beads between entanglements was estimated as $N_e \approx 90$. This is slightly higher than the value of $N_e \approx 86$ reported by Hoy *et al.*²⁹

D. Primitive path analysis

A slightly modified version of the annealing method of Everaers *et al.*² was used to obtain the primitive paths (PPs) and is briefly summarized. The end beads of the LPs were held stationary in the simulation box, while all other beads were free to move within the extent permitted by the FENE bonds and pairwise LJ interactions. Temperature rescaling was turned off, and a viscous dissipative force given in Eq. (4) was applied to each bead to slowly drain the energy of the system.

$$\mathbf{F}_d = -\gamma\mathbf{v}. \quad (4)$$

Here, the damping coefficient was set as $\gamma = 1$ (the choice of γ does not significantly affect the results of the PP analysis, as it is essentially an energy minimization). The energy and extent of intrachain pairwise interactions (ϵ and σ) were reduced linearly to zero in a short period of time $\approx 2.5\tau$, while interchain pairwise interactions were kept unchanged. Since the minimum of the FENE potential is at $r = 0$, a melt of LPs will slowly evolve toward a state where the chains pull themselves taut. From a practical standpoint, however, it would take infinite time for a system to reach this minimum energy configuration. Thus, the system was allowed to evolve (without temperature rescaling) until the temperature dropped below $10^{-3}\epsilon/k_B$. The FENE bonds were then replaced by stiff harmonic bonds with a potential given in Eq. (5).

$$U_{\text{harmonic}}(r) = \frac{K}{2}(r - R_h)^2. \quad (5)$$

The parameters of the stiff harmonic bond were set as $R_h = 0$; $K = 600\epsilon/\sigma^2$. This resulted in the polymer chains be-

TABLE I. Summary of molecular weight (N), number of polymers (N_p), and mean square radius of gyration (R_g^2) for the systems studied. The number density for all simulations is $\rho=0.85\sigma^{-3}$. The average bond length and characteristic ratio were obtained as $b=0.965\pm 0.002\sigma$ and $C_\infty=1.77\pm 0.03$.

N	Brute-force		SMWD	
	N_p	R_g^2	N_p	R_g^2
LPs				
64	50	17.16 ± 1.0	200	17.23 ± 0.1
128	50	37.42 ± 2.3	200	36.04 ± 0.2
256	50	77.82 ± 4.8	200	74.15 ± 0.3
512	50	153.25 ± 10.9	200	152.00 ± 0.4
1024	50	283.33 ± 18.1	200	289.24 ± 1.5
CPs				
64	50	8.43 ± 0.3	50	8.22 ± 0.3
128	50	15.65 ± 0.6	50	16.82 ± 0.6
256	50	29.53 ± 1.4	50	30.16 ± 1.2
512	50	49.26 ± 2.1	50	53.99 ± 2.0
1024	50	90.78 ± 3.9	50	88.01 ± 3.6
2048	50	147.53 ± 5.8
4096	50	244.72 ± 9.7
8192	50	400.11 ± 16.2

ing pulled taut, and the resulting polymer contours were taken to be the primitive paths. The average number of entanglements Z , and the average number of beads per entanglement N_e were then computed as

$$Z = \frac{L_{pp}^2}{R_{ee}^2}, \quad N_e = \frac{N}{Z}, \quad (6)$$

where L_{pp} is the mean contour length of the primitive paths.

The CPs in this study are nonconcatenated and unknotted. Annealing a system of pure CPs, as performed by Subramanian and Shanbhag,³⁰ where none of the beads of a CP are permanently fixed, would lead to all CPs in the system collapsing to a single point, and thus, the primitive path analysis was not performed on CPs. It must be noted here that it is nevertheless possible to perform PP analysis for CPs by fixing, for example, two diametrically opposite beads, but this is the topic of some debate, as the notion of primitive path for CPs is somewhat poorly defined.

III. RESULTS

The subscripts L and C are used to distinguish between quantities pertaining to LPs and CPs, respectively. All simulations were executed using LAMMPS,³¹ with a few custom modifications. The systems simulated in this study are summarized in Table I, along with the mean square radius of gyration of the polymers. For all systems, the simulation box size is at least twice R_g . Figure 2 shows a plot of decay of the autocorrelation function for LPs and CPs with molecular weight $N=1024$ over the course of brute-force equilibration. CPs were seen to relax faster than LPs, and the configurations obtained after $p_i(t)$ had decayed past zero were considered fully equilibrated. The average bond length in these systems was then measured as $b=0.965\pm 0.002\sigma$. The char-

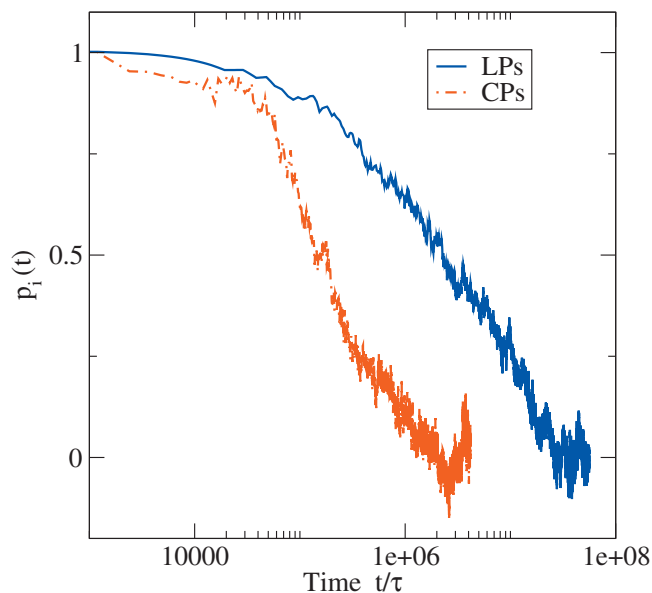


FIG. 2. Decay of the autocorrelation function defined in Eq. (3) during brute-force equilibration for LPs and CPs with molecular weight $N=1024$.

acteristic ratio was obtained as $C_\infty=1.77\pm 0.03$ by fitting the mean square radius of gyration data for LPs obtained using brute-force equilibration to the expression³²

$$[R_g^2]_L = \frac{1}{6}C_\infty b^2(N-1). \quad (7)$$

These values for the average bond length and characteristic ratio are consistent with values obtained previously.^{1,13} This indicates that for purposes of studying static properties, the number of polymers in each system is sufficient, and that the systems are well-equilibrated. It is corroborated by the results on the internal length scales, and primitive path statistics, presented later on in this section. Nevertheless, it must be noted that measuring dynamic properties of these systems might produce artifacts resulting from polymers interacting with themselves other across the periodic boundaries.

A. Polymer dimensions and entanglement statistics

The overall size of the polymers generated in this study is given in Table I. LPs display a Gaussian scaling of size, and for both LPs and CPs, the results from both equilibration methods are in good agreement. Figure 3 shows a plot of R_{ee}^2 and R_g^2 for CPs. The scaling of CP size follows $[R_g^2]_C \sim N^{2\nu}$, where $\nu \approx 0.4$ for low molecular weights, and seems to asymptotically approach $\nu \approx 1/3$ for large N . (The actual fits obtained are $[R_g^2]_C \sim N^{0.84\pm 0.02}$ for $N \leq 1024$, and $[R_g^2]_C \sim N^{0.69\pm 0.01}$ for $N > 1024$.) This confirms the scaling seen in other studies.^{11,12}

In addition to the overall size, polymer conformations at all length scales can be probed simultaneously by computing the mean square internal distance between beads. For a system with molecular weight N , let $\mathbf{R}(i)$ and $\mathbf{R}(j)$ denote the coordinates of beads i and j , respectively, ($i > j$) of the same polymer. Setting $n=(i-j)$, the mean square internal distance at scale n is given as

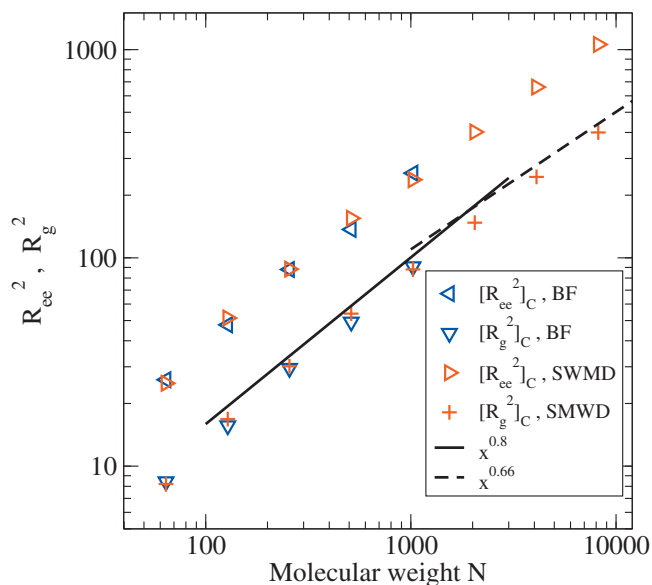


FIG. 3. Dimensions of CPs generated in this study using brute-force equilibration (BF) and SMWD. The solid line is $y=x^{0.8}$ and the broken line is $y=x^{0.66}$.

$$R^2(n) = \langle [\mathbf{R}(i) - \mathbf{R}(j)] \cdot [\mathbf{R}(i) - \mathbf{R}(j)] \rangle, \quad (8)$$

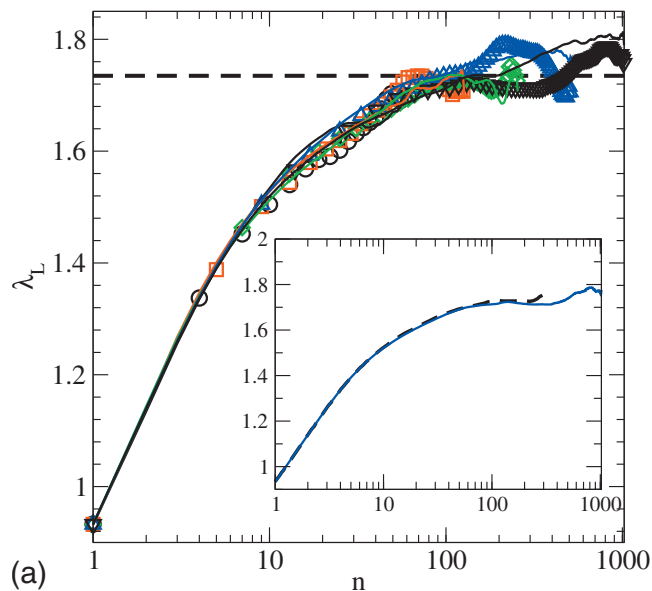
where the average is computed over all possible beads i and j that belong to a polymer with $n=i-j$, over all polymers in the system. Analytically, the mean square internal distance for Gaussian LPs and CPs (Ref. 32) is given as

$$\lambda_L = \frac{[R^2(n)]_L}{n} = C_\infty b^2, \quad (9)$$

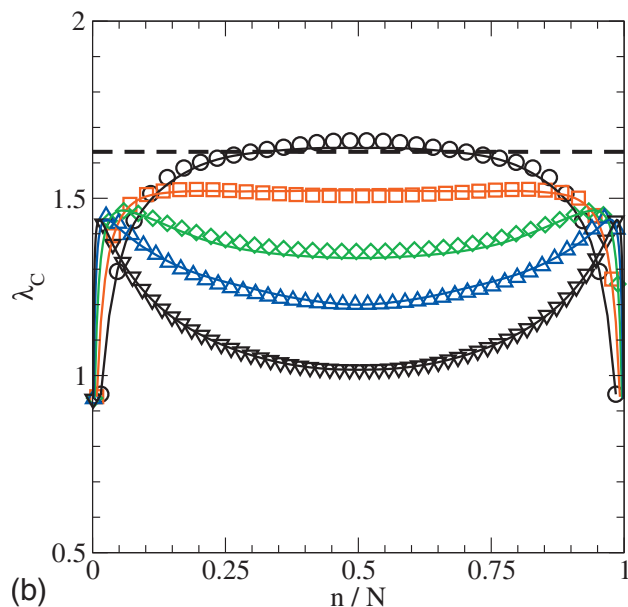
$$\lambda_C = \frac{[R^2(n)]_C}{n(1-n/N)} = C_\infty b^2. \quad (10)$$

Plots of λ_L and λ_C obtained from both equilibration methods are shown in Figs. 4(a) and 4(b), respectively. The inset of Fig. 4(a) shows the results obtained for $N=1024$ in SMWD, along with the so-called target function used by Auhl *et al.*^{13,33} For CPs, in order to collapse the results from all molecular weights onto the same horizontal axis, λ_C is plotted as a function of n/N . The results obtained from both equilibration methods are in good agreement. The noncatenation constraint imposed on the CPs manifests itself as a “pressure” that increases with molecular weight,^{34–36} forcing CPs to adopt compact conformations. LPs, on the other hand, are not subjected to the same topological constraints and therefore display Gaussian behavior at all but the smallest length scales.

Figure 5 shows a plot of N_e , the average number of beads between entanglements, obtained by PP analysis of LP melts generated using both equilibration methods. Also shown are values of N_e obtained from studies that use the bead-spring model with the same parameters used in this study and the same annealing PP analysis. For LPs generated using both equilibration methods, the number of beads between entanglements seems to asymptotically approach $N_e \approx 90$.



(a)



(b)

FIG. 4. Plot of the mean square internal distance between beads for (a) LPs [inset: target function obtained by Auhl *et al.* (Ref. 13) (broken line), along with the results for $N=1024$ (solid line)] and (b) CPs. In the main figures, symbols denote melts generated by brute-force equilibration and solid lines denote melts generated by SMWD. Broken black lines denote the Gaussian expectation. The molecular weights are 64 (\circ), 128 (\square), 256 (\diamond), 512 (\triangle), and 1024 (∇).

B. Evolution of quantities in the transition period

As mentioned previously, the transition period of SMWD is the period over which a newly generated polymer system of molecular weight N_{new} is allowed to evolve and reach equilibrium. At the beginning of the transition period, $t=0$, the system with molecular weight N_{new} has just been generated, and the polymers are maximally deformed. For well-equilibrated Gaussian LPs, the radii of gyration of the two different molecular weights are related by $R_g^2(N_{\text{new}}) = 2R_g^2(N_{\text{old}})$ or a factor of 2. The affine scaling that generates N_{new} from N_{old} changes R_g by a factor of $2^{1/3}$, or equivalently changes R_g^2 by a factor of $2^{2/3}$. Thus, in the transition period,

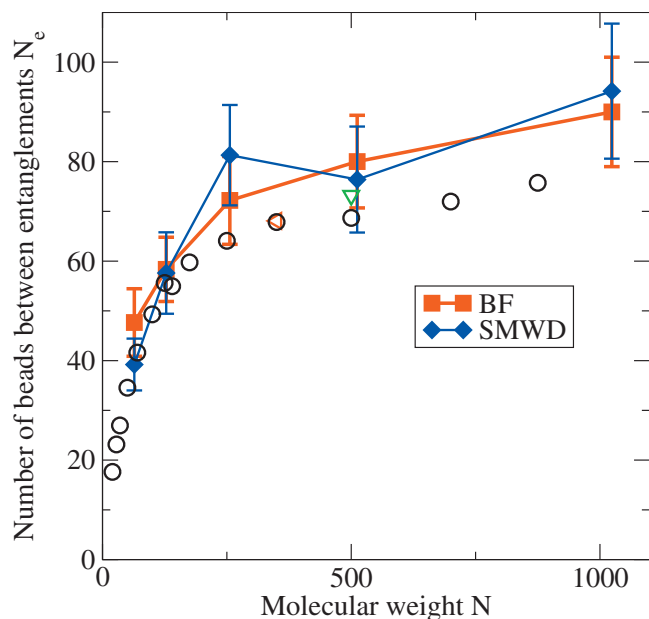


FIG. 5. Average number of beads between entanglements, N_e , obtained from PP analysis of melts generated in this study (filled symbols). Also shown (open symbols) are N_e values seen in the literature by Zhou and Larson (\ominus) (Ref. 37), Hoy, Foteinopoulou, and Kröger (\circ) (Ref. 38), and Hoy and Robbins (∇) (Ref. 29).

for large t , the ratio $R_g^2(t)/R_g^2(t=0)$ should approach $2^{1/3}$. Figure 6 shows the evolution of the mean square radius of gyration over the transition period. The ratio $R_g^2(t)/R_g^2(t=0)$ seems to reach the expected value of $2^{1/3} \approx 1.26$ in a period on the order of one Rouse time and fluctuates about the mean.

The evolution of the internal length scales also follows a scaling similar to the mean square radius of gyration. The affine scaling increases all length scales by the factor $2^{1/3}$. The internal length scales of a polymer melt before and after the scaling (at $t=0$) are given by

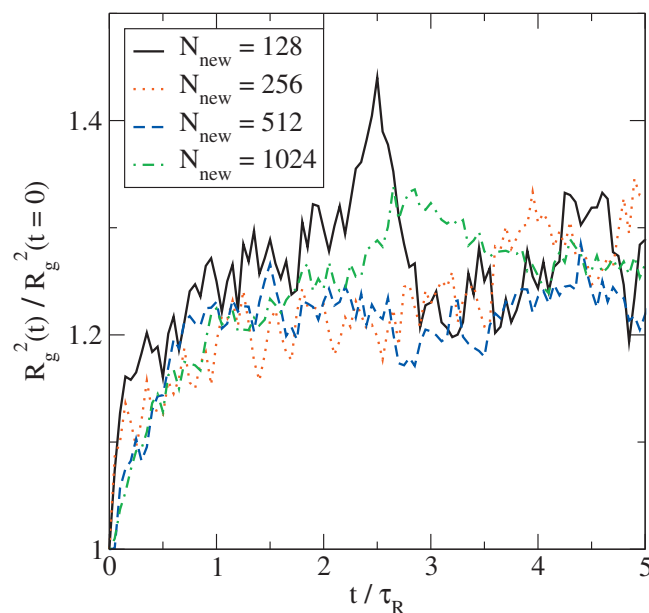


FIG. 6. Evolution of the mean square radius of gyration of LPs over the transition period. The ratio $R_g^2(t)/R_g^2(t=0)$ seems to reach a value ≈ 1.26 in approximately one Rouse time.

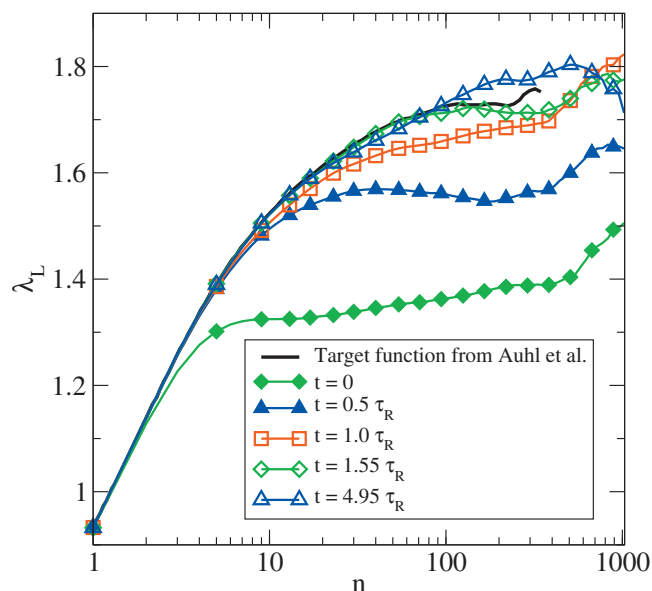


FIG. 7. The evolution of the internal length scales over the transition period for LPs with $N_{\text{new}}=1024$ generated by SMWD (a) λ_L at various values of t . The Gaussian nature of LPs at all but the smallest length scales develops in a time on the order of one Rouse time and seems to fluctuate about the mean.

$$\left[\frac{R^2(n)}{n} \right]_{\text{new}} = 2^{2/3} \left[\frac{R^2(n)}{2n} \right]_{\text{old}} = 2^{-1/3} \left[\frac{R^2(n)}{n} \right]_{\text{old}}. \quad (11)$$

This corresponds to the plateau of λ_L being scaled down by 26% due to the affine scaling, which is corrected during the transition period. Figure 7 shows a plot of λ_L for the molecular weight $N=1024$ at a few selected values of t , along with the target function from Auhl *et al.*¹³ It is seen that the LPs generated by SMWD are maximally deformed (by 26%) at all length scales at $t=0$, and expand to reach their equilibrium conformation in a time on the order of one Rouse time. The smaller scales seem to reach equilibrium before the larger scales. The equilibrium conformation is Gaussian at all but the smallest length scales, and fluctuates about the mean as the simulations are continued beyond one Rouse time.

Figure 8 shows the variation of the average number of entanglements on LPs over the course of the transition period. The number of entanglements reaches equilibrium in approximately one Rouse time and fluctuates about the mean. However, the actual value of $Z(t)/Z(t=0)$ is less than 2 for lower molecular weights and seems to approach 2 as N increases. This behavior is consistent with the expectation that for polymers with $N \gg N_e$, with a doubling of molecular weight; the ratio $Z(t)/Z(t=0)$ is expected to approach a value of 2.

For low-molecular weight CPs, on the other hand, for large t , the ratio $R_g^2(t)/R_g^2(t=0)$ is expected to reach approximately 1.09. For higher molecular weights, this ratio is unity, and the desired increase in CP dimensions is produced by the affine scaling alone. For CPs generated using SMWD, as the number of polymers was $N_p=50$, this 9% (or less) increase in size was not significant enough to be reliably detected, and thus, these results are not shown. However, the internal structure of the CPs undergoes rearrangement, as evidenced

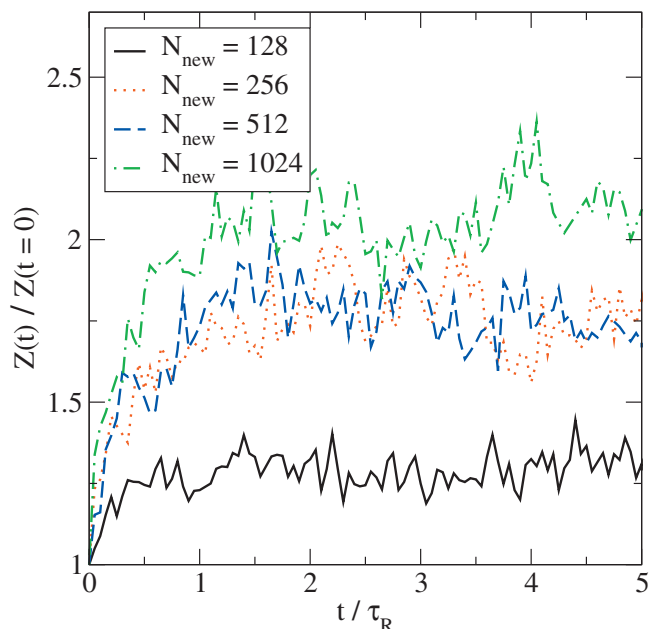


FIG. 8. Evolution of the average number of entanglements on LPs during the transition period. For large N , a doubling of molecular weight leads to a doubling of Z in approximately one Rouse time.

by the mean square internal distance between beads. Figure 9 shows a plot of λ_C as a function of n/N for the molecular weight $N=1024$ at three different values of t . This intermediate molecular weight was chosen because it is large enough to be entangled and small enough to allow for sufficient averaging at all length scales. The solid black line shows the results obtained from melts of CPs generated by brute-force equilibration. At the beginning of the transition period, the conformations of newly generated CPs are somewhat close to equilibrium and slowly evolve to reach their equilibrium conformations in a time on the order of one Rouse time.

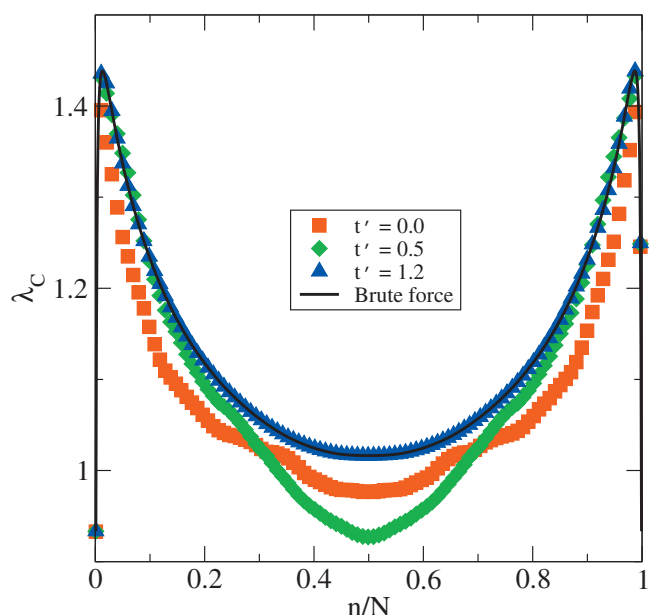


FIG. 9. The evolution of the internal distance between beads during the transition period for CPs with molecular weight $N_{\text{new}}=1024$. The solid black line indicates CPs obtained by brute-force equilibration in this study.

IV. DISCUSSION

The transition period for SMWD was originally thought to be on the order of a Rouse time of an LP of molecular weight N_{new} . Looking at the evolution of polymer dimensions and entanglement statistics, the reason for this choice becomes somewhat clearer. The affine scaling used in the SMWD method preserves the large-scale random walk nature of polymers in the melt, albeit with the incorrect scaling of the end-to-end distance (this error is about 26% for LPs and significantly lower for CPs). At the beginning of the transition period, polymers are thus more compact than their equilibrium counterparts. In a mean field sense, an LP at the beginning of the transition period is constrained to move within the confines of the tube formed by preexisting entanglements. The compact nature of LPs, coupled with the constraints posed by the tube drives an LP to expand along the tube. From the point of view of entanglements, LPs at the beginning of the transition period have approximately half as many entanglements as their equilibrium counterparts. New entanglements are expected to introduce themselves in between preexisting entanglements by the ends of other polymers in the melt, in a manner which is the opposite of constraint-release.^{39,40} Conversely, the segment of the chain between pre-existing entanglements is free to move within the constraints posed by the self-avoiding nature of the beads and is unhindered by the presence of entanglements.

Thus, in a time on the order of τ_R , the segments of the chains between pre-existing entanglements are expected to reach equilibrium. The data presented in Figs. 6–9 all bear out this expectation with regard to internal length scales and number of entanglements on a chain. A melt of pure CPs, on the other hand, is unentangled and has faster dynamics than a melt of pure LPs. Therefore, the transition period for pure CPs is less than the transition period for pure LPs.

The total time required by the successive molecular weight doubling method, $\tau_{\text{total}}(N)$, to generate an equilibrated melt of polymers with molecular weight N can now be estimated. The molecular weight of the seed configuration for the first stage of SMWD is denoted by N_o and the molecular weight at stage i is given by

$$N_i = 2^i N_o. \quad (12)$$

If the total number of stages is denoted by m , the final molecular weight N is obtained by setting $i=m$ in the above expression. At each stage, the duration of the transition period is on the order of the Rouse time of the molecular weight N_i , given by

$$\tau_R(N_i) \approx \tau_e \left(\frac{N_i}{N_e} \right)^2. \quad (13)$$

Neglecting the time taken to generate the seed configuration with molecular weight N_o , and the time taken to scale the simulation box and add beads, the total time is the sum of the time taken for each transition period, and can be written as

$$\tau_{\text{total}}(N) = \sum_{i=1}^m \tau_R(N_i) = \left[\tau_e \left(\frac{N_o}{N_e} \right)^2 \right] \sum_{i=1}^m 2^{2i}. \quad (14)$$

The terms in the summation on the right hand side form a geometric progression, and for $2^{2m} \gg 1$, the total time can be written as

$$\tau_{\text{total}}(N) = \left[\tau_e \left(\frac{N_o}{N_e} \right)^2 \right] \frac{4}{3} (2^m)^2 = \frac{4}{3} \tau_R(N) \sim N^2. \quad (15)$$

This expression also indicates that tripling or quadrupling the molecular weight at each stage might not produce a significant speed-up, as only the prefactor associated with the total time changes.

While the data presented here all seem to indicate the viability of the SMWD method, it is important to mention outstanding issues and possible sources of error that may need further investigation. Judging the quality of equilibration of a polymer melt is a complex, many-body problem. This study has used only three of a variety of possible metrics to compare equilibration methods. The metrics used in this study are, at the time of writing, three of the most common metrics used to characterize polymer structure, and for LPs, λ_L is considered an extremely robust metric. Nevertheless, it is possible that other metrics might indicate that the SMWD method may not yield good quality melts, and that a transition period different from τ_R might be required for each stage.

Secondly, the segment of the polymer chain between preexisting entanglements is assumed to be capable of moving freely. Strictly speaking, as the affinely scaled configuration evolves, entanglements will introduce themselves in the originally free segment, hindering its motion. However, these new entanglements are thought to be introduced by chain ends, and therefore, the hindrance to motion should not be significant. Thus, the proper transition period might be a multiple of the Rouse time. It is also possible that by some mechanism similar to the slow melting that produces heterogeneous melts, the proper transition period might scale with the molecular weight to a power higher than 2.

Finally, the distribution of entanglements along a polymer chain and the mechanism by which entanglements introduce themselves over the course of the transition period are two topics that warrant further investigation. Since the purpose of this paper is to outline the SMWD method and establish the relevant computational framework, these topics are delegated to a future study.

V. CONCLUSIONS

A new, topology-preserving method for the generation of equilibrated polymer melts was presented. This successive molecular weight doubling method was used to generate melts of linear and cyclic polymers. Melts generated by SMWD were compared with melts generated by brute-force equilibration. As indicated by the metrics used in this study, the quality of melts generated by both methods is comparable. For the molecular weights considered in this study, the SWMD method generates equilibrated polymer melts (along with all intermediate molecular weights) in simulation time

that scales as N^2 , as opposed to brute-force methods that scale as $N^{3.4}$ for linear polymers, and is thought to be applicable to a variety of polymer architectures.

ACKNOWLEDGMENTS

The author wishes to express his gratitude to Professor Sachin Shanbhag for extremely insightful discussions on polymers, and MC and MD methods. Thanks to Professor Rahmi Ozisik and Professor R. Catalin Picu for many useful suggestions and criticisms. Special thanks to Mr. Tim Wickberg for his patience and expert maintenance of the SCOREC computing clusters. Thanks also to Renge Li, Zhi Li, Nithin Mathew, Ali Shahsavari, and Ardavan Zandiatashbar for their inputs throughout the course of this study. Part of the simulations was executed on the SUR BlueGene/L at Rensselaer Polytechnic Institute, which is supported by NSF Grant No. 0420703, and a gift by the IBM Corporation of a BlueGene/L computer.

- ¹K. Kremer and G. S. Grest, *J. Chem. Phys.* **92**, 5057 (1990).
- ²R. Everaers, S. K. Sukumaran, G. S. Grest, C. Svaneborg, A. Sivasubramanian, and K. Kremer, *Science* **303**, 823 (2004).
- ³Q. Zhou and R. G. Larson, *Macromolecules* **39**, 6737 (2006).
- ⁴R. Hoy and M. Robbins, *J. Chem. Phys.* **131**, 244901 (2009).
- ⁵T. Vettorel and K. Kremer, *Macromol. Theory Simul.* **19**, 44 (2010).
- ⁶D. MacNeill and J. Rottler, *Phys. Rev. E* **81**, 011804 (2010).
- ⁷I. Dukovski and M. Muthukumar, *J. Chem. Phys.* **118**, 6648 (2003).
- ⁸J. I. McKechnie, D. Brown, and J. H. R. Clarke, *Macromolecules* **25**, 1562 (1992).
- ⁹M. Müller, J. Nievergelt, S. Santos, and U. W. Suter, *J. Chem. Phys.* **114**, 9764 (2001).
- ¹⁰T. Vettorel, S. Y. Reigh, D. Y. Yoon, and K. Kremer, *Macromol. Rapid Commun.* **30**, 345 (2009).
- ¹¹T. Vettorel, A. Y. Grosberg, and K. Kremer, *Phys. Biol.* **6**, 025013 (2009).
- ¹²J. Suzuki, A. Takano, T. Deguchi, and Y. Matsushita, *J. Chem. Phys.* **131**, 144902 (2009).
- ¹³R. Auhl, R. Everaers, G. S. Grest, K. Kremer, and S. J. Plimpton, *J. Chem. Phys.* **119**, 12718 (2003).
- ¹⁴D. Brown, J. H. R. Clarke, M. Okuda, and T. Yamazaki, *J. Chem. Phys.* **100**, 6011 (1994).
- ¹⁵N. C. Karayiannis, V. G. Mavrantzas, and D. N. Theodorou, *Phys. Rev. Lett.* **88**, 105503 (2002).
- ¹⁶I. Carmesin and K. Kremer, *Macromolecules* **21**, 2819 (1988).
- ¹⁷J. S. Shaffer, *J. Chem. Phys.* **101**, 4205 (1994).
- ¹⁸N. C. Karayiannis, A. E. Giannousaki, and V. G. Mavrantzas, *J. Chem. Phys.* **118**, 2451 (2003).
- ¹⁹L. D. Peristeras, I. G. Economou, and D. N. Theodorou, *Macromolecules* **38**, 386 (2005).
- ²⁰J. Gao, *J. Chem. Phys.* **102**, 1074 (1995).
- ²¹M. Perez, O. Lame, F. Leonforte, and J. L. Barrat, *J. Chem. Phys.* **128**, 234904 (2008).
- ²²S. K. Sukumaran, G. S. Grest, K. Kremer, and R. Everaers, *J. Polym. Sci., Part B: Polym. Phys.* **43**, 917 (2005).
- ²³P.-G. deGennes, *C. R. Acad. Sci. Paris* **321**, 363 (1995).
- ²⁴S. Rastogi, L. Kurelec, J. Cuijpers, D. Lippits, M. Wimmer, and P. J. Lemstra, *Macromol. Mater. Eng.* **288**, 964 (2003).
- ²⁵S. Rastogi, D. R. Lippits, G. W. Peters, R. Graf, Y. Yao, and H. W. Spiess, *Nature Mater.* **4**, 635 (2005).
- ²⁶D. R. Lippits, S. Rastogi, S. Talebi, and C. Bailly, *Macromolecules* **39**, 8882 (2006).
- ²⁷G. Subramanian and S. Shanbhag, *Int. J. Multiscale Comp. Eng.* **7**, 55 (2009).
- ²⁸G. Subramanian and S. Shanbhag, *Macromolecules* **41**, 7239 (2008).
- ²⁹R. S. Hoy, K. Foteinopoulou, and M. Kröger, *Phys. Rev. E* **80**, 031803 (2009).
- ³⁰G. Subramanian and S. Shanbhag, *Phys. Rev. E* **77**, 011801 (2008).
- ³¹S. Plimpton, *J. Comput. Phys.* **117**, 1 (1995).
- ³²B. H. Zimm and W. H. Stockmayer, *J. Chem. Phys.* **17**, 1301 (1949).

- ³³J. P. Wittmer, P. Beckrich, H. Meyer, A. Cavallo, A. Johner, and J. Baschnagel, *Phys. Rev. E* **76**, 011803 (2007).
- ³⁴M. E. Cates and J. M. Deutsch, *J. Phys. (Paris)* **47**, 2121 (1986).
- ³⁵B. V. S. Iyer, A. K. Lele, and S. Shanbhag, *Macromolecules* **40**, 5995 (2007).
- ³⁶G. Subramanian and S. Shanbhag, *Phys. Rev. E* **80**, 041806 (2009).
- ³⁷Q. Zhou and R. G. Larson, *Macromolecules* **38**, 5761 (2005).
- ³⁸R. S. Hoy and M. O. Robbins, *Phys. Rev. E* **72**, 061802 (2005).
- ³⁹P.-G. deGennes, *J. Phys. (France)* **36**, 1199 (1975).
- ⁴⁰P.-G. deGennes, *Macromolecules* **9**, 587 (1976).